Hydrodynamic Stability and Natural Convection in Ostwald-de Waele and Ellis Fluids: The Development of a Numerical Solution

An algorithm was developed for the finite-difference computation of hydrodynamic stability and natural convection in non-Newtonian fluids heated from below. Test calculations were carried out for fluids whose viscosity characteristics are described by the Ostwald-de Waele (power-law) and Ellis models and for roll-cells with both rigid and dragless vertical boundaries. The effects of time-step and grid-size were tested thoroughly. The results were found to be independent of the assumed initial state. The computed values of the Nusselt number and the critical Rayleigh number for Newtonian fluids agree well with prior experimental results. The computations for the Ostwald-de Waele model indicate that the approximate solution of Tien, Tsuei, and Sun may underestimate the critical Rayleigh Number.

HIROYUKI OZOE and STUART W. CHURCHILL

School of Chemical Engineering
University of Pennsylvania
Philadelphia, Pennsylvania 19104

SCOPE

When a fluid is heated from below at low temperature differences, heat transfer is by conduction alone. However, above some critical temperature gradients, a circulatory motion is the stable state. The onset of this circulation as the critical gradient is exceeded may generate significant forces on the wall of a storage tank and may cause rapid boiling in a saturated fluid. Either of these events may cause failure of the tank. The stable circulation which is eventually attained increases the rate of heat transfer which may also be of practical importance. Since the critical conditions for the onset of motion depend on a balance of the viscous, buoyant, and inertial forces in the liquid, the behavior of non-Newtonian fluids, whose viscosity depends on the motion itself, cannot necessarily be inferred from the well-known behavior of Newtonian fluids. The objective of this investigation was to develop theoretical solutions to be used for the prediction of this behavior.

The theoretical solution requires that the mode of the motion be postulated. Concurrent experimental work indicated that the stable mode of circulation in a long horizontal channel of rectangular cross section is a series of two-dimensional, horizontal rolls with their axes perpendicular to the length of the channel. This same motion is observed between horizontal plates although the rolls are not then so perfectly aligned. If significant heat leakage occurs through the side walls the motion may instead consist of a single roll with its axis parallel to the length of the channel. Accordingly, solutions were developed for both of these two modes.

Two rheological models were chosen to simulate the behavior of pseudoplastic fluids—the Ostwald-de Waele or power-law model and the Ellis model. The former has the advantage of simplicity and mathematical tractability and hence has been utilized in most theoretical investigations of pseudoplastic behavior. However it does not converge to Newtonian behavior in the limit of zero rate of strain which would be presumed to be of critical importance in this problem. The Ellis model behaves correctly in this limit, and fluids such as dilute aqueous solutions of carboxymethylcellulose and polyethylene oxide are well represented over the entire range of the rate of strain encompassed in this investigation. The disadvantage of the Ellis model is that it involves three empirical constants and provides an implicit relationship between the rate of strain and the shear stress. Both of these models imply that elastic effects may be neglected. The limits of applicability of this assumption are to be investigated in future work.

Although there have been many prior investigations of hydrodynamic instability and natural convection in Newtonian fluids and a few investigations of free (unconfined) convection in non-Newtonian fluids the only prior work on the combined problem is by Tien, Tseui, and Sun (1969) who presented an approximate solution and some experimental data. The results herein are compared with this prior work.

The mathematical model was solved in real time by finite-difference methods therefore predicting the transient as well as the steady state behavior. The solutions encompass a wide range of non-Newtonian behavior and a moderate range of conditions above the critical temperature difference.

Correspondence concerning this paper should be addressed to S. W. Churchill. H. Ozoe is with Okayama University, Okayama, Japan.

CONCLUSIONS AND SIGNIFICANCE

The solutions for the critical Rayleigh number and for the relationship between the Nusselt number and the Rayleigh number agree well with prior solutions and experimental results for the limiting case of Newtonian fluids. Values computed using the Ellis model agree reasonably with those computed for the equivalent Ostwald-de Waele model. The prior experimental results for non-Newtonian fluids are not of sufficient precision to provide a critical test of these solutions for non-Newtonian fluids. However, the agreement of the results for Newtonian fluids, the convergence of the solutions with decreasing grid-size and the general structure of the computed values suggests that they are probably valid for fluids whose rheological behavior can be represented by the Ostwald-de Waele or Ellis models. The computational procedure developed in this study would require only minor modification for most other rheological models but remains to be tested for elastic effects.

The computational procedure yields the transient as well as the steady state behavior. Calculations for different initial conditions all converged to the same final state and revealed no hysteresis.

The principal shortcoming of the procedure is the excessive computational time required to establish independence from grid-size. The empirical correlation permits extrapolation of results obtained with a relatively large grid-size and hence in a moderate computing time to zero grid-size. However, further improvement of the computational algorithm to avoid the necessity and uncertainty of this extrapolation is desirable. The computation of the steady heat flux within the region instead of at the walls as proposed by deVahl Davis is not a cureall for the problem of finite grid-size.

The results presented herein provide the basis for the development in a subsequent paper of an empirical correlation for the prediction of the Nusselt numbers as a function of Rayleigh numbers for any pseudoplastic fluid whose shear stress is known as a function of the rate of strain.

This work is a continuation of a long range research program on the development of methods for the prediction of natural convection by numerical integration of the partial differential equations of conservation as reviewed by Churchill (1966). Hellums and Churchill (1961, 1962) first developed an explicit procedure for the numerical solution of these equations for both a heated, vertical plate and the region inside a long, circular, horizontal cylinder heated on one vertical, curved side and cooled on the other. Wilkes and Churchill (1966) next developed an implicit procedure for the more complex flow field in a long, horizontal, rectangular channel heated on one vertical side and cooled on the other. Samuels and Churchill (1967) modified this method to calculate the circulation in a long, horizontal rectangular channel heated from below and cooled from above and hence determined the critical conditions for circulation. Their solutions agreed with the analytical solutions obtained by Kurzweg (1965) by linearization for large Pr but revealed a different dependence on Pr for small Pr. Numerical methods of solution have also been developed by Aziz and Hellums (1967) and Chorin (1966) for the critical conditions for two- and three-dimensional circulations in regions heated from below.

The objective of this investigation was to develop a computational procedure for the circulation and the critical conditions for circulation in non-Newtonian fluids in the expectation that the behavior might differ significantly from that of Newtonian fluids. No single model appears to represent the behavior of all non-Newtonian fluids. Furthermore, the various models each involve two or more coefficients as contrasted with the single coefficient (viscosity) required for Newtonian fluids. Hence it is not feasible to compute the convective behavior of all fluids for all parametric conditions. Attention was therefore given to the development of an algorithm for computation which could be used with as many fluid models as possible. The Ostwald-de Waele (power-law) and Ellis models were chosen as representative of the behavior of non-Newtonian fluids for illustrative calculations—the former because of its simplicity and widespread use as a model in other processes and the latter because of the better representation of the behavior of real fluids. Some fluids demonstrate a variation in the effective viscosity with time following the application of a shear stress. This complexity is neglected in the models and formulations considered herein.

Based on the experimental observations of Samuels and Churchill (1967) and Ozoe (1971) two modes of circulation were chosen for the calculations. The first mode is a single two-dimensional roll-cell in a long, horizontal channel with a square cross section and hence with zero velocity and finite drag on all four walls as illustrated in Figure 1. The second mode is a two-dimensional roll-cell in a square region with no drag on the vertical sides. This roll-cell corresponds to an interior roll-cell in a row of roll-cells with axes normal to the axis of the channel as illustrated in Figure 2 and also to a roll-cell in the region between infinite horizontal plates.

The only directly related, prior work appears to be that of Tien, Tsuei, and Sun (1969) who developed an analytical solution for only the critical Rayleigh number of an

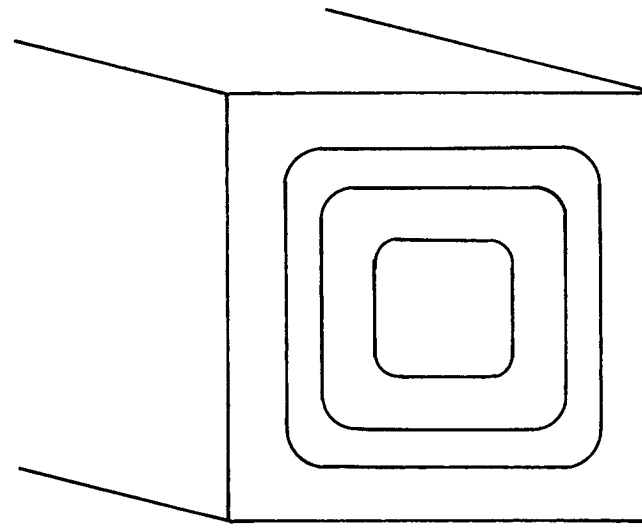

Fig. 1. Two-dimensional roll-cell with drag on all four walls.

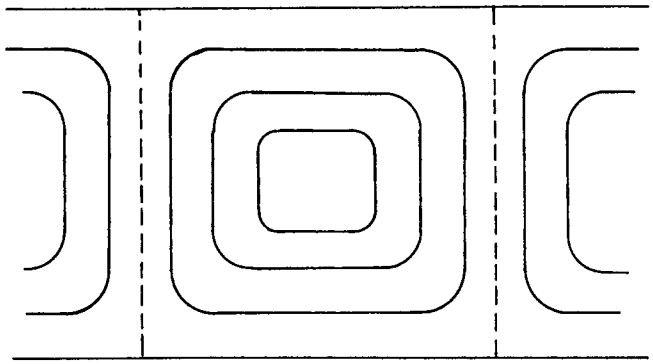

Fig. 2. Two-dimensional roll-cell with no drag on vertical boundaries.

Ostwald-de Waele fluid between infinite horizontal plates heated from below and cooled from above. Their solution is based on the energy principle for stability and utilizes the circulation pattern of a Newtonian fluid. They presented experimental data for the critical Rayleigh number for solutions of carboxymethylcellulose (CMC) in water. Tsuei (1970) reported experimental values of the Nusselt numbers above the critical value.

In this paper attention is focused on the development and verification of the computational procedure since many of the computational experiences and findings are believed to be relevant and applicable to the development of numerical solutions for other convective phenomena. The application of the numerical results to the prediction of the behavior of fluids which do not follow the Ostwald-de Waele model has been described in Ozoe and Churchill (1972). Further details on the work reported herein are also given by Ozoe (1971).

MATHEMATICAL MODEL

Making the following significant assumptions:

1. Two-dimensional motion
2. Negligible dissipation
3. Negligible variation in physical properties other than density
4. $\rho = \rho_0/[1 + \beta(T - T_0)]$
5. $\beta(T - T_0) << 1$

which are known as the Boussinesq approximation permits expression of the equations for the conservation of material, momentum, and energy in the following form:

$$\frac{\partial u}{\partial x} + \frac{\partial v}{\partial y} = 0 \tag{1}$$

$$\rho_0\left(\frac{\partial u}{\partial t} + u\frac{\partial u}{\partial x} + v\frac{\partial u}{\partial y}\right) = -\frac{\partial p'}{\partial x} + \eta\left(\frac{\partial^2 u}{\partial x^2} + \frac{\partial^2 u}{\partial y^2}\right) + 2\frac{\partial \eta}{\partial x}\frac{\partial u}{\partial x} + \frac{\partial \eta}{\partial y}\left(\frac{\partial v}{\partial x} + \frac{\partial u}{\partial y}\right) \tag{2}$$

$$\rho_0\left(\frac{\partial v}{\partial t} + u\frac{\partial v}{\partial x} + v\frac{\partial v}{\partial y}\right) = -\rho_0 g\beta(T - T_0) - \frac{\partial p'}{\partial y} + \eta\left(\frac{\partial^2 v}{\partial x^2} + \frac{\partial^2 v}{\partial y^2}\right) + 2\frac{\partial \eta}{\partial y}\frac{\partial v}{\partial y} + \frac{\partial \eta}{\partial x}\left(\frac{\partial v}{\partial x} + \frac{\partial u}{\partial y}\right) \tag{3}$$

$$\frac{\partial T}{\partial t} + u\frac{\partial T}{\partial x} + v\frac{\partial T}{\partial y} = K\left(\frac{\partial^2 T}{\partial x^2} + \frac{\partial^2 T}{\partial y^2}\right) \tag{4}$$

The Ostwald-de Waele model for the relationship between the velocity field and the shear stress may be expressed in terms of the effective viscosity in Equations (2) and (3) as follows for this reduced case:

$$\eta = m\left|\left(2\left[\left(\frac{\partial u}{\partial x}\right)^2 + \left(\frac{\partial v}{\partial y}\right)^2\right] + \left[\frac{\partial u}{\partial y} + \frac{\partial v}{\partial x}\right]^2\right)^{1/2}\right|^{n-1} \tag{5}$$

The boundary conditions for solid vertical walls are

$$u(0, y, t) = u(l, y, t) = u(x, 0, t) = u(x, h, t) = v(x, 0, t) = v(x, h, t) = 0 \tag{6}$$

$$v(0, y, t) = v(l, y, t) = 0 \tag{7}$$

$$T(x, 0, t) = T_C \tag{8}$$

$$T(x, h, t) = T_H \tag{9}$$

$$\frac{\partial T}{\partial x}(0, y, t) = \frac{\partial T}{\partial x}(l, y, t) = 0 \tag{10}$$

For dragless vertical boundaries, conditions (7) are replaced by

$$\frac{\partial v}{\partial x}(0, y, t) = \frac{\partial v}{\partial x}(l, y, t) = 0 \tag{11}$$

Equations (1) to (11) may be simplified and written in dimensionless form by the procedure of Hellums and Churchill (1964), yielding for Equations (1) to (5)

$$U_X + V_Y = 0 \tag{12}$$

$$\frac{1}{Pr}[U_\tau + UU_X + VU_Y] = -P_X' + 2H_X U_X + H_Y(U_Y + V_X) + H(U_{XX} + U_{YY}) \tag{13}$$

$$\frac{1}{Pr}[V_\tau + UV_X + VV_Y] = -Ra\,\theta - P_Y' + 2H_Y V_Y + H_X(U_Y + V_X) + H(V_{XX} + V_{YY}) \tag{14}$$

$$\theta_\tau + U\theta_X + V\theta_Y = \theta_{XX} + \theta_{YY} \tag{15}$$

$$H = \left|(2[U_X^2 + V_Y^2] + [U_Y + V_X]^2)^{1/2}\right|^{n-1} \tag{16}$$

and equivalent expressions for Equations (6) to (11) where here the two dimensionless parameters have the special definitions:

$$Pr = mh^{2-2n}/\rho_0 K^{2-n} \tag{17}$$

$$Ra = \rho_0 g\beta(T_H - T_C)h^{2n+1}/mK^n \tag{18}$$

For $n = 1$: $\eta = m = \mu$, $H = 1$ and Pr and Ra reduce to the conventional expressions for a Newtonian fluid.

Differentiating Equations (13) and (14) by Y and X, respectively, and subtracting eliminates the pressure. Defining a dimensionless stream function such that

$$\Psi_Y = U \tag{19}$$

and

$$\Psi_X = -V \tag{20}$$

and a dimensionless vorticity

$$\zeta = V_X - U_Y = -[\Psi_{XX} + \Psi_{YY}] \tag{21}$$

permits replacement of Equations (12), (13), and (14) by the vorticity equation

$$\frac{1}{Pr}(\zeta_\tau + U\zeta_X + V\zeta_Y) =$$

$$-Ra\,\theta_X + H(\zeta_{XX} + \zeta_{YY}) + (H_{XX} - H_{YY})(V_X + U_Y)$$
$$- 2H_{XY}(U_X - V_Y) + 2(H_X\zeta_X + H_Y\zeta_Y) \quad (22)$$

For solid vertical walls the stream function has the same value on all four boundaries and this value can arbitrarily be chosen as zero. For dragless vertical boundaries the vorticity as well as the stream function is zero on the two vertical walls since V_X, U, and U_Y are zero. Initial conditions for ζ, Ψ, U, V, and θ must be chosen to complete the description.

The above formulation is convenient for solution for $Pr \geq 1$ since the inertial terms vanish as $Pr \to \infty$. For $Pr \leq 1$ it is convenient to use an alternate set of dimensionless variables for which $Ra/Pr^{\frac{n}{2-n}}$ rather than Ra appears as multiplier of θ_X in the vorticity equation and $Pr^{\frac{1}{2-n}}$ as a multiplier of the convective terms in the energy equation rather than Pr as a multiplier of the inertial terms in the vorticity equation. This representation is described by Ozoe (1971) but is omitted here since primary interest is in fluids for which $Pr \geq 1$. For $Pr = 1$ the two representations become identical.

METHOD OF SOLUTION

The steady state solution, which is of primary interest, might be obtained by dropping the time derivatives. If a 10×10 subdivision were then used for finite-difference calculations there would be 99 unknown temperatures and 117 unknown vorticities for solid vertical walls. For dragless vertical walls the unknown vorticities are reduced to 99. The resulting 198×198 or greater matrix might be solvable with the available computing facilities but the truncation error would probably be excessive.

Alternatively the unsteady state equations might be solved in small increments of time until a steady state were attained. Wilkes and Churchill (1966) and Samuels and Churchill (1967) attained a steady state using the Alternating-Direction-Implicit (ADI) method and this procedure was used herein. The method requires the solution of 20 tridiagonal 9×9 matrices two times in one direction and 9 11×11 plus 9 9×9 in the other at each time-step. The nonlinearity of the equations precludes advance determination of the maximum stable time-step, if any. However, a stable time-step was determined for many conditions by trial and error. From an arbitrary, steady, or unsteady state the system was perturbed by a step-change in physical properties, geometry or motion, and the equations integrated numerically to another steady state.

Finite Difference Formulation

The derivatives in X and Y were approximated by second-order finite differences. A forward, first-order difference was used for the derivatives of time and a second-order central difference for the components of velocity. The modification of the ADI method by Brian (1961) was used to lower the truncation error. Details of the formulation are given by Ozoe (1971).

Calculation Procedure

The temperature field was first computed from the energy equation and then the vorticity field from the vorticity equation using values of the vorticity at the wall, and the velocity and stream-function fields from the previous time-step. The stream-function field was then calculated from the internal vorticity field. The new vorticities at the wall were calculated from the stream function by extrapolation. The calculation of the vorticity at the wall and the stream function could be repeated iteratively at each time-step until convergent values were obtained. However this iteration is not necessary if only the steady state solution is sought. Except for one trial calculation, only a single iteration was used in this work.

The stream function was first calculated from the finite-difference form of Equation (21) by the relaxation method but convergence was found to be rather slow. This calculation was speeded up by following the lead of Samuels and Churchill (1967) and adding a transient term. The fictitious time-step $\Delta\tau^*$ is unrelated to $\Delta\tau$ and a value of $\Delta\tau^* = 6(\Delta X)^2$ was used.

The fourth-order Taylor expansion was used for calculation of the velocity components from the stream-function following the experience of Wilkes and Churchill (1966) who found the fourth-order approximation more accurate than the second-order one. At points adjacent to the wall the third-order approximation was used. For dragless vertical boundaries the V-velocity along the side was calculated by extrapolation of the internal values of the stream function using the third-order Taylor expansion. The fourth-order expansion did not give significantly different results.

The Nusselt number along the upper wall:

$$Nu(0) = (\theta_Y)_{Y=0} \quad (23)$$

was calculated using the second-order Taylor expansion for θ_Y since it gave consistently higher values than the third-order approximation. The Nusselt number obtained by finite-difference computations is notoriously inaccurate owing to the uncertainty of the temperature gradient at the wall. Following the suggestion of deVahl Davis (1970) the Nusselt number at other elevations in the channel was calculated from the temperature gradient and the convective flux as follows in the hope of obtaining greater accuracy:

$$Nu(Y) = \theta_Y - V\theta \quad (24)$$

The average Nusselt number across the cell was found by integration using the second-order Simpson method for odd numbers of grid points and the trapezoidal approximation for even numbers. At steady state the average Nusselt number should be independent of the elevation. $\overline{Nu}$ is independent of the choice of the reference velocity since the average velocity is zero across the channel.

Formulation and Procedure for the Ellis Model

The Ellis model for the relationship between the velocity field and the shear stress may be expressed in terms of the effective viscosity in Equations (2) and (3) as follows in dimensional and dimensionless form:

$$\frac{1}{\eta} = \phi_0 + \phi_1 \left| \left(2\left(\frac{\partial u}{\partial x}\right)^2 + 2\left(\frac{\partial v}{\partial y}\right)^2 + \left(\frac{\partial v}{\partial x} + \frac{\partial u}{\partial y}\right)^2\right)^{1/2} \right|^{\alpha-1} \tau^{\alpha-1} \quad (25)$$

$$\frac{1}{H} = \Phi_0 + \Phi_1 \left|\left((2U_X^2 + 2V_Y^2 + (V_X + U_Y)^2\right)^{1/2}\right|^{\alpha-1} H^{\alpha-1} \quad (26)$$

Equation (26) was solved for H at each grid point and time by the Newton-Raphson method using the values of the velocity components at the previous time-step. Otherwise the procedure of calculation was the same as for the Ostwald-de Waele model.

CALCULATIONS

Ostwald-de Waele Model—Solid Vertical Boundaries

Calculations were first carried out using the alternative dimensionless representation for $Pr \leq 1$. All calculations were carried out for $\Delta X = \Delta Y = 0.1$ and $\Delta\tau = 0.001$ except as noted to the contrary. The steady state temperature and velocity fields obtained by Samuels (1966) for a Newtonian fluid with $Pr = 0.1$ and $Ra = 6000$ were used as an initial condition for the first calculations. A step change to $Pr = 1$ and $Ra = 6000$ was made and the steady state obtained for this new Newtonian case. A step change to $n = 0.9$ at the same Pr and Ra was next tried. The dimensionless viscosities at the corners were assigned an arbitrary value of 10^4 since the Ostwald-de Waele model gives an infinite viscosity as the velocity gradients approach zero, which is unacceptable in the computer program. This procedure resulted in numerical instability. However, when the corner viscosities were assigned the average of the values obtained by second-order extrapolation along both walls a stable calculation was obtained.

The transient response of $\overline{Nu}(0)$ to a step change from the Newtonian steady state at the same values of Pr and Ra is illustrated in Figures 3 and 4. Curve 1 in Figure 3 for $n = 0.9$ shows a rapid convergence to the steady state. Curve 1 in Figure 4 for $n = 0.8$ also converges rapidly. Curve 3 in Figure 3 for $n = 0.6$ indicates numerical instability but reduction of Pr produced convergence as indicated by Curve 4 in Figure 3. This procedure did not succeed for $n \leq 0.4$ as indicated by Curves 3 and 4 in Figure 4. For conditions yielding a value of $\overline{Nu}$ near unity convergence was slow as indicated by Curve 2 in Figure 4. Curve 2 in Figure 3 shows slow and uncertain convergence as would be expected for large Pr using the dimensionless representation designed for $Pr \leq 1$.

Since the two dimensionless representations become identical for $Pr = 1$, the steady state solutions obtained with the alternative representation were used as starting values for calculations with the regular representation. $Pr = 10$ was chosen as an example of large Pr since the difference between $Pr = 10$ and $Pr \to \infty$ would be expected to be negligible based on results of Samuels and Churchill (1967) with Newtonian fluids. To test this presumption for the formulation herein the left side of Equation (22) was dropped for a test calculation at $Ra = 6000$. The resulting value of $\overline{Nu}(0)$ was 1.994 as compared to 1.992 for $Pr = 10$. A larger value of Pr would require more calculation time since the rate of response decreases with increasing Pr.

A step change from $Pr = 1$ to 10 produced numerical instability but a series of steps in Pr and the use of a smaller $\Delta\tau$ produced convergence to the steady state. Rapid convergence was also obtained from the Newtonian solution for $Pr = 10$ and $Ra = 6000$ to $n = 0.9$ at the same Pr and Ra. For $n = 0.8$, 0.7, 0.6 and 0.5, Ra was decreased in steps to cover the range $1 \leq \overline{Nu}(0) \leq 2.5$. The computations for $n \leq 0.4$ converged very slowly and the results are not considered reliable.

A change from one value of n to a smaller value produced a drastic change in $\overline{Nu}(0)$. In order to try to improve convergence, n and Ra were changed simultaneously to produce almost the same value of $\overline{Nu}(0)$ as the initial value. However, the velocity field still changed drastically, the response curve was unnatural, and convergence was not improved significantly.

For large time-steps the velocity field changed radically

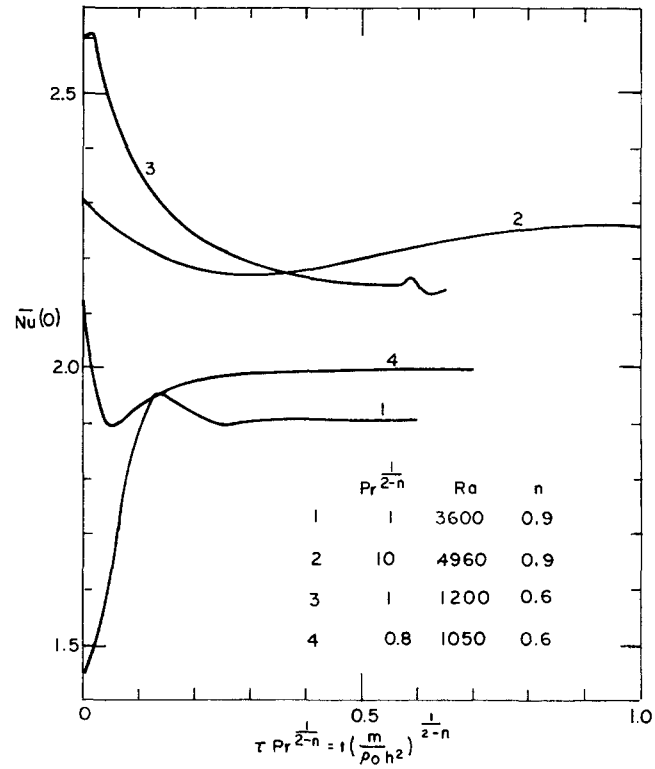

Fig. 3. Transient response of $\overline{Nu}(0)$ for Ostwald-de Waele fluids and solid vertical boundaries.

$\Delta X = \Delta Y = 0.1$

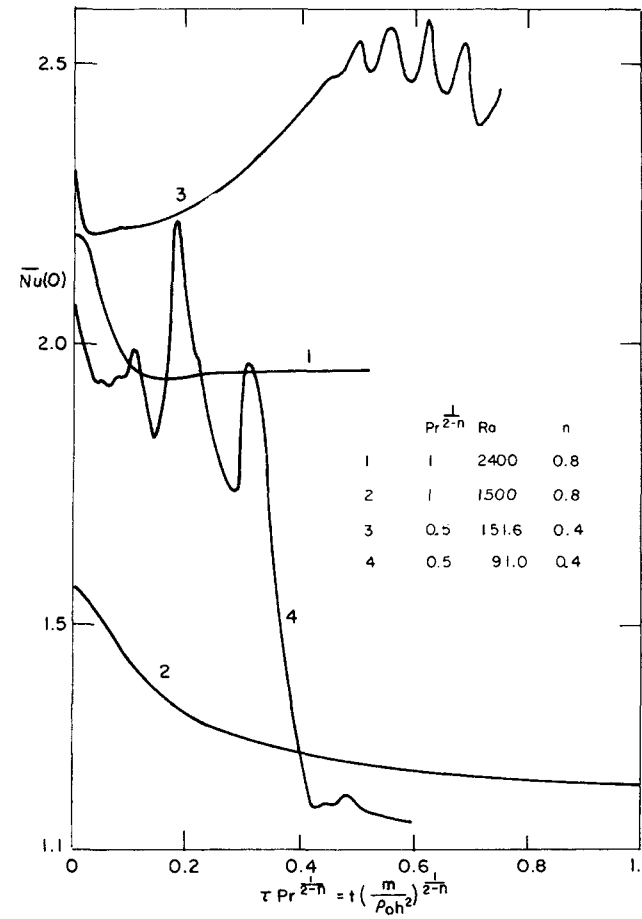

Fig. 4. Transient response of $\overline{Nu}(0)$ for Ostwald-de Waele fluids and solid vertical boundaries.

$\Delta X = \Delta Y = 0.1$

and the number of iterations required to solve for the stream function increased. Decreasing the time-step moderately actually decreased the computing time under some circumstances. For example for $n = 0.6$, $Pr = 10$, and $Ra = 720$ the required number of iterations decreased from 10-12 to 2-3 as $\Delta\tau$ was decreased from 10^{-3} to 5×10^{-4} resulting in approximately a 50% reduction in computing time.

The computed values of $\overline{Nu}(0)$ for $Pr = 10$ are plotted in Figure 5. The values computed for $Pr = 1$ by both representations differ only slightly from those for $Pr = 10$. The computed values of Samuels and Churchill (1967) for $Pr \geq 1$ agree well with the values computed herein for $Pr = 10$ and $n = 1.0$. Hence Figure 5 can be considered to represent all $Pr > 1$. The critical Rayleigh number Ra_c is obtained by extrapolation of the curves to $\overline{Nu}(0) = 1.0$.

Ostwald-de Waele Model—Dragless Vertical Boundaries

Calculations for this case and $Pr = 10$ were carried out starting from the steady state solution for solid vertical walls for the same conditions. In each case $\overline{Nu}(0)$ first increased abruptly and then converged in a smooth oscillation. The rate of convergence was rapid for $Ra >> Ra_c$ but was slow as $Ra \rightarrow Ra_c$. For $Ra << Ra_c$ the calculations converged rapidly to the static state. Convergence to the steady state was confirmed not only by the Nusselt number at the upper wall but also by the central stream function which responds more rapidly to a change in conditions.

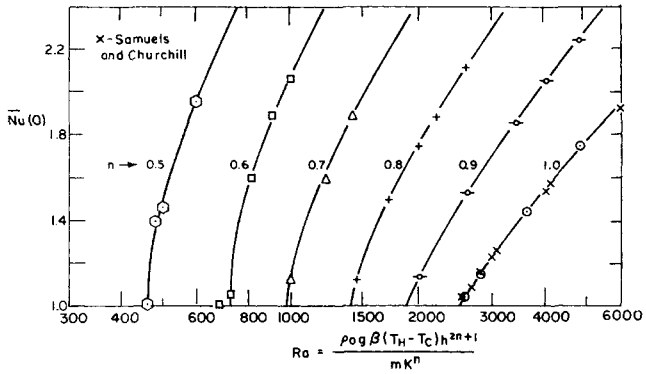

Fig. 5. Steady $\overline{Nu}(0)$ for Ostwald-de Waele and Newtonian fluids and solid vertical boundaries.

$\Delta X = \Delta Y = 0.1$, $Pr = 10$

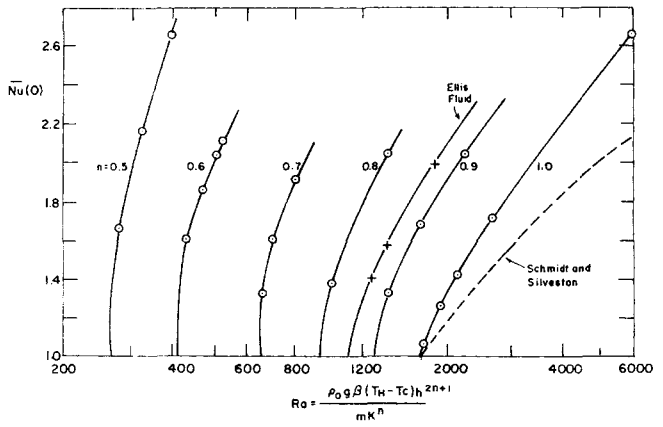

Fig. 6. Steady $\overline{Nu}(0)$ for Newtonian, Ostwald-de Waele and Ellis fluids and dragless vertical boundaries.

$\Delta X = \Delta Y = 0.1$, $Pr = 10$

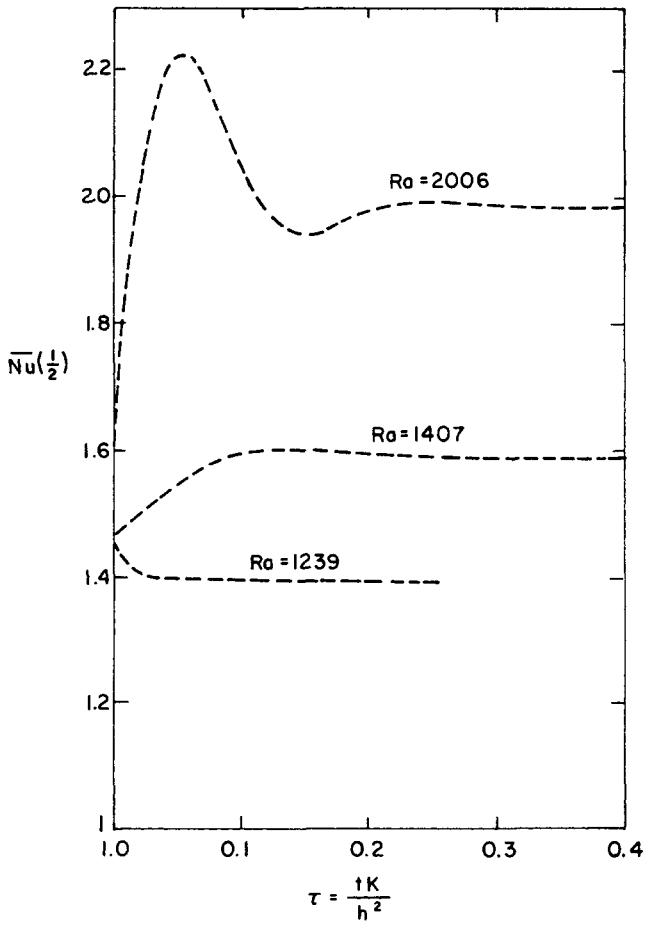

Fig. 7. Transient response of $\overline{Nu}\left(\frac{1}{2}\right)$ for an Ellis fluid and dragless vertical boundaries.

$\Delta X = \Delta Y = 0.1$, $Pr = 2.95$

The steady state results for $\Delta X = \Delta Y = 0.1$ are plotted in Figure 6. The computed values of $n = 1$ are higher than the curve representing the experimental results of Schmidt and Silveston (1959) except in the limit as $Ra \rightarrow Ra_c$ and $\overline{Nu}(0) \rightarrow 1$. This discrepancy is discussed later.

Ellis Model

To test the computational procedure for the Ellis model the following dimensionless coefficients, corresponding roughly to the values given by Bird, Stewart, and Lightfoot (1960) for 4% CMC solution, were used: $\Phi_0 = 0.636$, $\Phi_1 = 0.644$ and $\alpha = 1.17$. The viscosity-versus-shear-stress curve for this Ellis fluid is equivalent to that of an Ostwald-de Waele fluid with $n = 0.875$ and $m = 0.2065$ N·s^n/m^2 over the range of σ from 0.8 to 44 N/m^2. This analogy together with values of $\rho_0 = 1000$ kg/m^3 and $K_0 = 1.6 \times 10^{-7}$ m^2/s yields an effective value of 2,950 for Pr. In preliminary calculations with $Ra = 1400$, $\Delta\tau \leq 2 \times 10^{-5}$ was required for stability. Hence $Pr = 2.95$ was used since previous calculations for Newtonian and Ostwald-de Waele fluids indicated that the steady state value of $\overline{Nu}(0)$ is insensitive to $Pr > 1$ for the same Ra, although the maximum, stable time-step and the rate of convergence increase as Pr decreases. For $Pr = 2.95$ the calculations were stable for $\Delta\tau = 10^{-3}$. The results for dragless vertical boundaries and three different values of Ra are shown in Figure 7. The steady state values are included in Figure 6. They fall between the curves for $n =$

0.8 and 0.9 and indicate the same trend with Ra as the results for the Ostwald-de Waele model.

Computational Time

The computations were carried out at the University of Pennsylvania Computing Center on an IBM-360/75. The integration required about 0.5 sec. for each time-step for the Newtonian model. For $\Delta X = \Delta Y = 0.10$ the required number of time-steps to attain the steady state varied from about 50 to 100, hence the total time was from about 25 to 50 seconds. For $\Delta X = \Delta Y = 0.05$ the required time-steps increased to as many as 1,100 and the total time to as much as 900 seconds. The time requirement did not increase significantly for the Ostwald-de Waele and Ellis models.

EVALUATION OF NUMERICAL CALCULATIONS

Dependence on Initial State

The calculations described above were generally started from a steady state close to the steady state to be computed in order to minimize the computing time. To provide a further test of the algorithm and to test the uniqueness of the previously computed steady states, several calculations were started from the conductive state. Since the conductive state is a solution of the equations, a fluctuation in temperature or velocity is necessary to generate a convective state. A central streamfunction of -20 with all other grid points at zero, corresponding to a central vortex, was imposed on the conductive state for a Newtonian fluid with dragless vertical boundaries $Pr = 10$, and $Ra = 6000$. As indicated in Figure 8 the Nusselt number at the middle elevation, $\overline{Nu}(\frac{1}{2})$ converged to 2.355 which agrees well with the value of 2.359 computed for another initial condition.

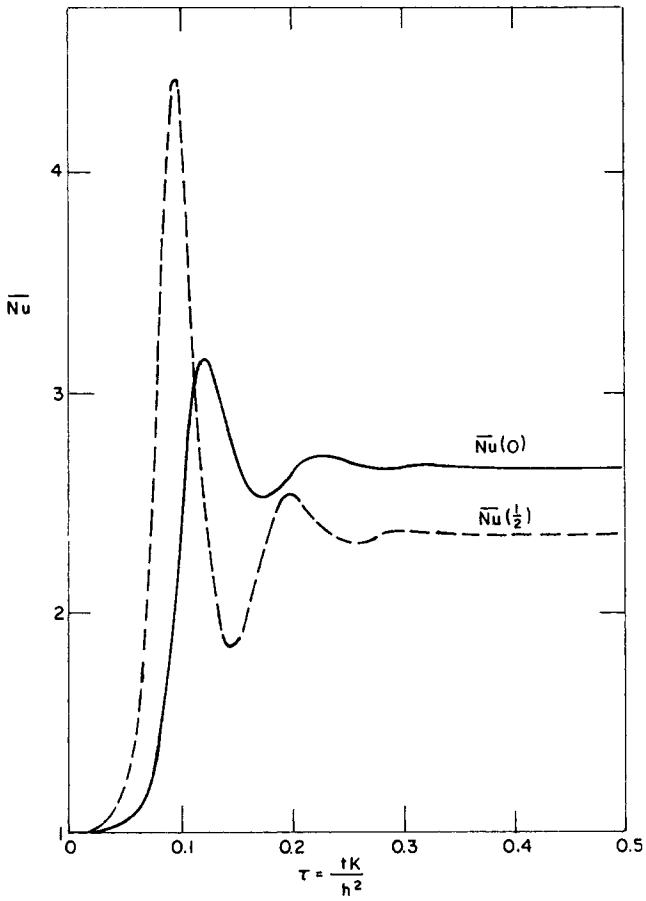

Fig. 8. Transient response of $\overline{Nu}$ from conductive state for a Newtonian fluid and dragless vertical boundaries.

$\Delta X = \Delta Y = 0.1$, $Ra = 6000$

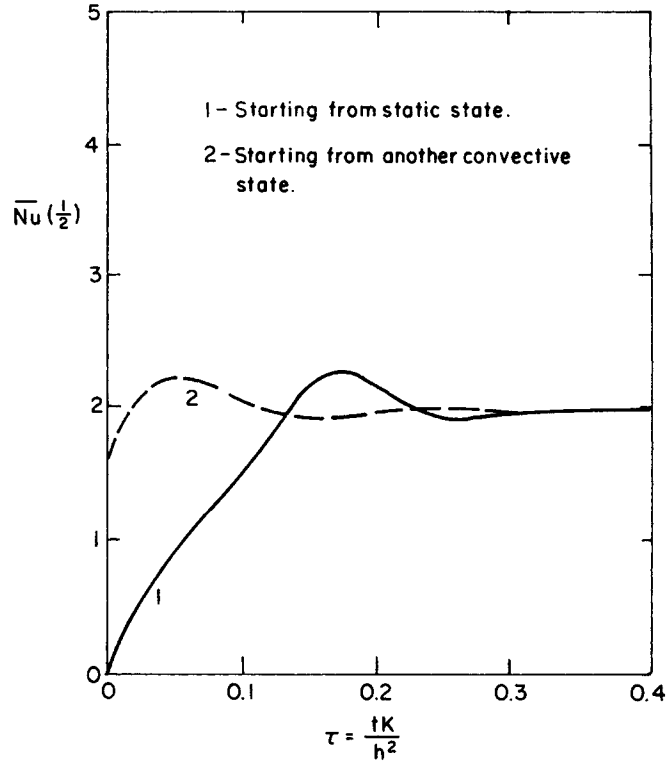

Fig. 9. Transient response of $\overline{Nu}$ from different initial states for an Ellis fluid and dragless vertical boundaries.

$\Delta X = \Delta Y = 0.1$, $Ra = 2006$, $Pr = 2.95$

The viscosity is not defined at the static state of zero shear-stress for the Ostwald-de Waele model. Hence the Ellis model with the same coefficients as before was used for additional calculations starting from the conductive state. $\overline{Nu}(\frac{1}{2})$ for dragless vertical boundaries is seen in Figure 9 to converge to the same steady, convective state starting from the conductive state and starting from another convective steady state. Figure 10 shows further calculations for dragless vertical boundaries starting from the conductive state for two values of Ra, one greater and one less than the critical value of 1160. For $Ra = 2006$, $\overline{Nu}(\frac{1}{2})$ is seen to converge to a steady, convective state. For $Ra = 1003$ convergence back to the conductive state of $\overline{Nu}(\frac{1}{2}) = 1$ occurs after an initial rise.

Effect of Time Step

Calculations were carried out for three different time-steps for dragless vertical boundaries with $n = 1.0$, $Pr = 10$, and $Ra = 2600$. For $\Delta\tau = 0.002$ numerical instability is evident in Figure 11 after 11 to 12 steps. However for $\Delta\tau = 0.001$ and 0.0005 instability did not develop and the computations converged to steady state values of $\overline{Nu}(\frac{1}{2}) = 1.625$ and 1.655, respectively, at times greater than those shown in Figure 11. It is concluded that the steady state Nusselt number is insensitive to the choice of $\Delta\tau$ as long as the computations are stable and hence that the discrepancy with the results of Schmidt and Silveston (1959) is not a function of the time-step. A value of $\Delta\tau = 0.001$ was subsequently first tried for non-Newtonian conditions but smaller values were used in those cases where instability manifested itself.

Effect of Elevation at Which $\overline{Nu}$ is Calculated

Figure 12 illustrates the result of computing $\overline{Nu}$ at various elevations using Equation (24). The fluctuation with height, which is similar to that obtained by Thomas (1970), indicates an error in the computations since the same value should be obtained at all elevations at steady state. Thomas used the average of the computed values at the different elevations.

Effect of Grid Size

To test the effect of grid-size, calculations were carried out at $\Delta X = \Delta Y = 0.05$ and 0.20 as well as 0.10. Figure 13 shows the transient behavior for dragless vertical boundaries, $n = 1$, $Pr = 10$ and $Ra = 2600$, first with $\Delta X = \Delta Y = 0.1$ starting from the steady solution for $Ra = 2100$ and $Pr = 10$. $\overline{Nu}(\frac{1}{2})$ approached an asymptotic value of 1.65 at $\tau = 0.25$. The grid-size was then changed to $\Delta X = \Delta Y = 0.05$ with initial values of the temperature and stream function for the intermediate points calculated by interpolation. $\overline{Nu}(\frac{1}{2})$ then approached an asymptotic value of 1.55 at $\tau = 0.47$. Hence it is clear that the previously computed values are not independent of grid-size. For the calculations with $\Delta X = \Delta Y = 0.1$, a value of $\Delta\tau = 10^{-3}$ was used. For $\Delta X = \Delta Y = 0.05$ it was necessary to reduce $\Delta\tau$ to 2×10^{-4} for stability and the net computing time was five times as great. To economize on computing time, calculations for the smaller subdivision were carried out only for a limited number of conditions and an empirical procedure was established for correction of the results for $\Delta X = \Delta Y = 0.10$.

Figure 14 demonstrates that the spurious fluctuation of $\overline{Nu}$ with height was due to too large a grid-size. More importantly the decrease in $\overline{Nu}$ as the grid-size decreases

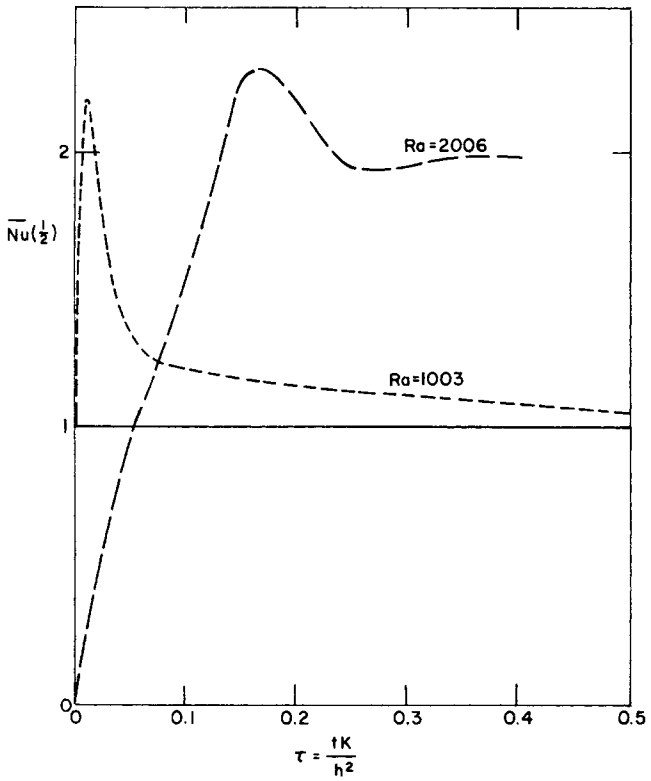

Fig. 10. Transient response of $\overline{Nu}\left(\frac{1}{2}\right)$ from the conductive state with Ra above and below Ra_c for an Ellis fluid and dragless vertical boundaries.

$\Delta X = \Delta Y = 0.1$, $Ra_c = 1160$

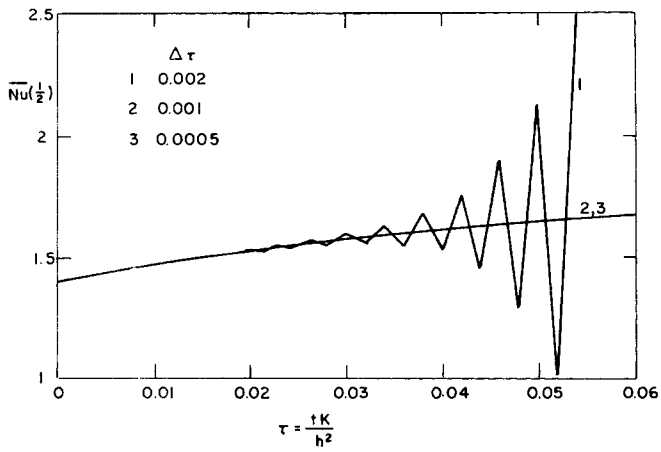

Fig. 11. Effect of time-step for a Newtonian fluid and dragless vertical boundaries.

$\Delta X = \Delta Y = 0.1$, $Ra = 2600$ $Pr = 10$

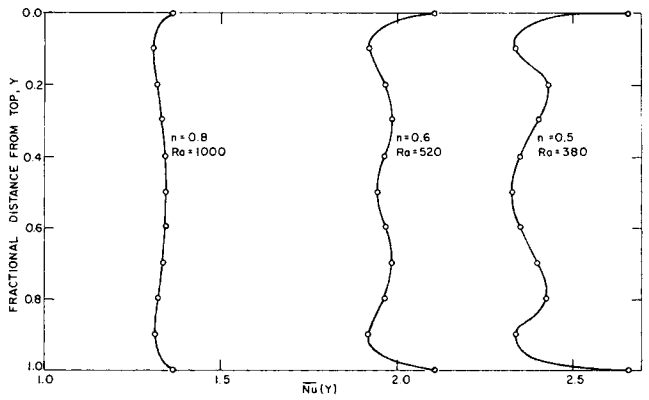

Fig. 12. Effect of elevation on calculated value of $\overline{Nu}$ for Ostwald-de Waele fluids and dragless vertical boundaries.

$\Delta X = \Delta Y = 0.1$, $Pr = 10$

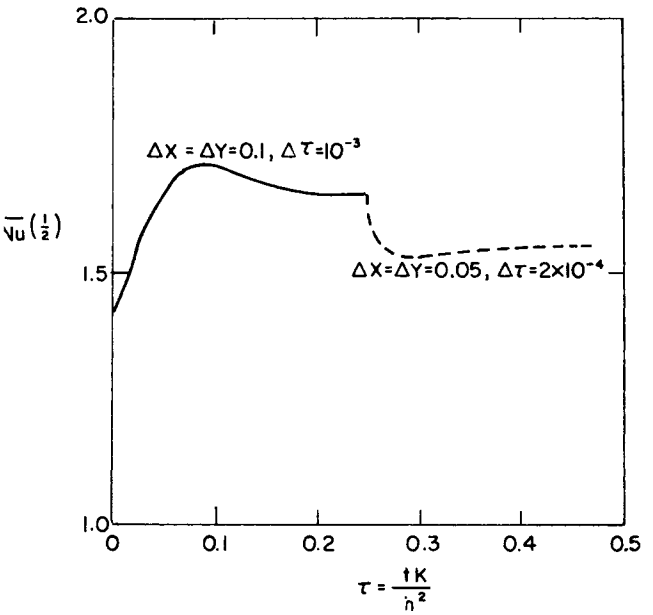

Fig. 13. Effect of grid size on transient response and steady state of $\overline{Nu}\left(\frac{1}{2}\right)$ for a Newtonian fluid and dragless vertical boundaries

$Ra = 2600$, $Pr = 10$

is greater than the fluctuation with height for the larger grid-size.

Figure 15 illustrates the extrapolation to zero grid-size for a number of conditions. As indicated the error for a finite grid-size increases with $\overline{Nu}$. This observation was used to construct the correlation in Figure 16 for the effect of grid-size. Figure 16, which is based only on calculations for $n = 0.5$ and 1.0 with dragless vertical boundaries, was used to correct all of the calculated values of $\overline{Nu}$ at $\Delta X = \Delta Y = 0.1$ to the equivalent values at $\Delta X = \Delta Y \rightarrow 0$.

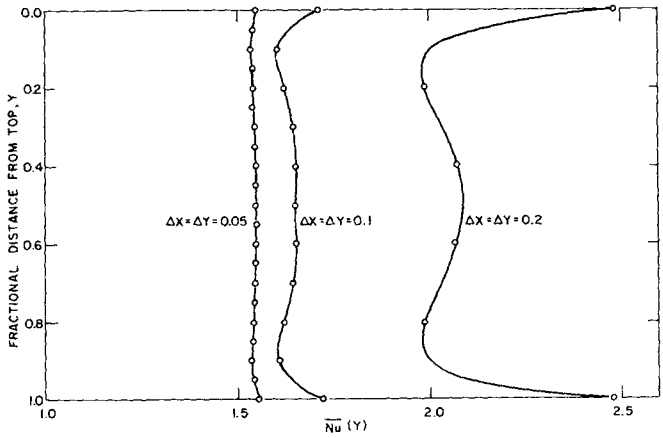

Fig. 14. Effect of grid size on calculation of $\overline{Nu}$ at different elevations for a Newtonian fluid and dragless vertical boundaries.

$Ra = 2600, Pr = 10$

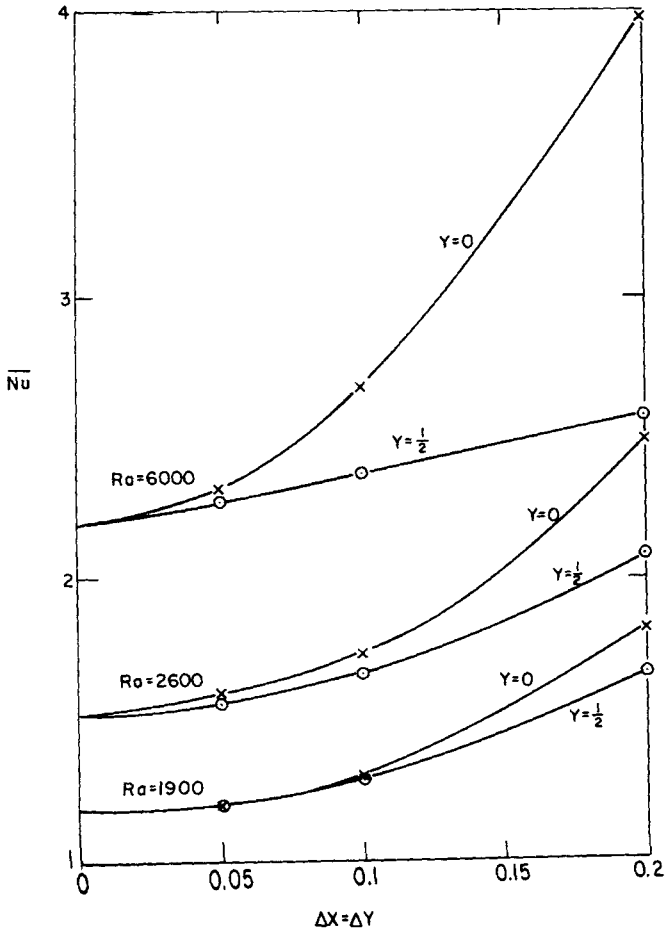

Fig. 15. Effect of grid size on $\overline{Nu}$ for a Newtonian fluid and dragless vertical boundaries.

Comparison with Prior Results

The corrected values for both dragless and solid vertical boundaries are plotted in Figures 17 and 18, respectively. The agreement of the corrected values for dragless vertical boundaries and $n = 1$ with the experimental correlation of Schmidt and Silveston (1959) and with the numerical results of Chorin (1966) is excellent. The computed values of Samuels and Churchill (1967) for solid boundaries were also for $\Delta X = \Delta Y = 0.1$. Correction of these values to $\Delta X = \Delta Y \rightarrow 0$ by Figure 16 would obviously maintain the close agreement demonstrated in Figure 5.

Tsuei (1970) obtained experimental values for various

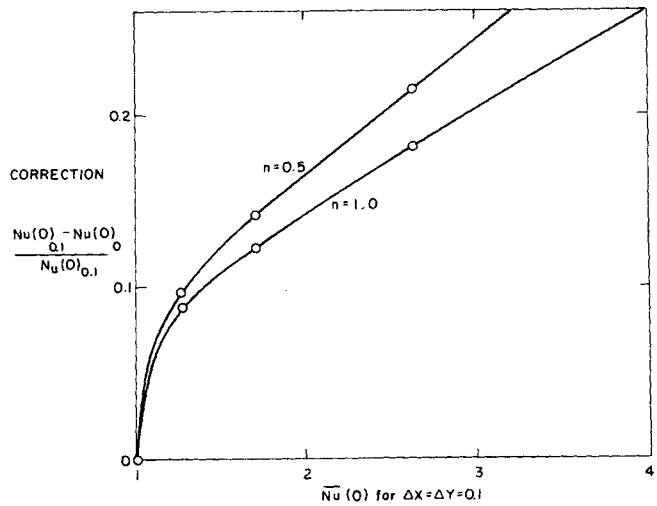

Fig. 16. Correlation for effect of grid size.

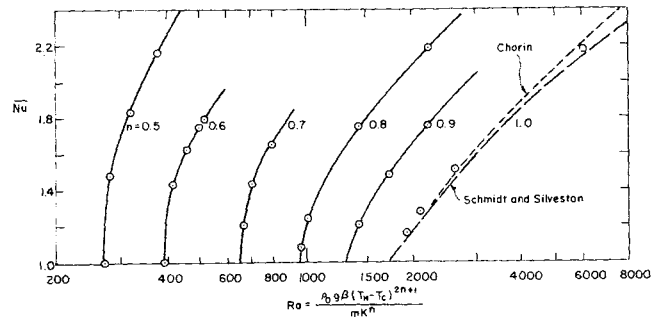

Fig. 17. $\overline{Nu}$ for Ostwald-de Waele and Newtonian fluids and dragless vertical boundaries—extrapolated to zero grid size.

$Pr > 1$

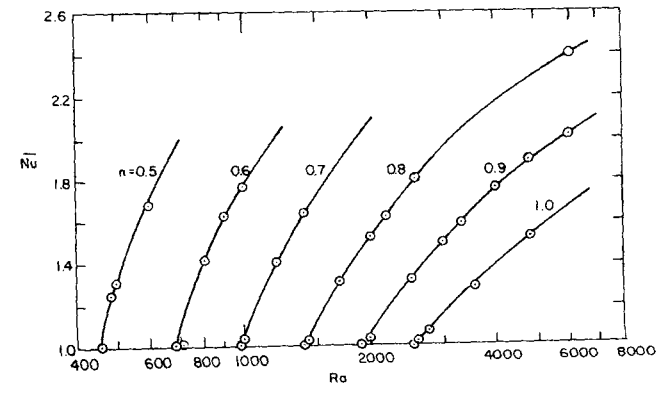

Fig. 18. $\overline{Nu}$ for Ostwald-de Waele and Newtonian fluids and solid vertical boundaries—extrapolated to zero grid size.

$Pr > 1$

non-Newtonian fluids which he modelled with the Ostwald-de Waele equation. His experimental results for 1.2% CMC-7HSP in water, for which he found a value of $n = 0.85$, and for glycerin, which is considered to be Newtonian, are compared with the results computed herein in Figure 19. The curve for $n = 0.85$ was obtained from Figure 17 by interpolation. His values scatter too much to provide a critical test of the computed values but the trends in $\overline{Nu}$ with Ra and n are in agreement.

Values of Ra_c for $Pr = 10$ and both solid and dragless boundaries are plotted versus n in Figure 20. These values were obtained by extrapolation of the values in Figures 5 and 6 to $\overline{Nu} = 1$ since Ra_c appears to be independent of grid-size. The solutions and experimental values of Tien, Tsuei, and Sun (1969) for Ra_c are compared with the values obtained herein for dragless vertical boundaries in Figure 21. The experimental values were obtained by extrapolation of data equivalent to those in Figure 19 and hence are not believed to be sufficiently accurate to provide a critical test of the theoretical solutions. The solutions obtained herein are presumed to be more accurate owing to their direct derivation from the equations of conservation. However, a final decision must await more precise data.

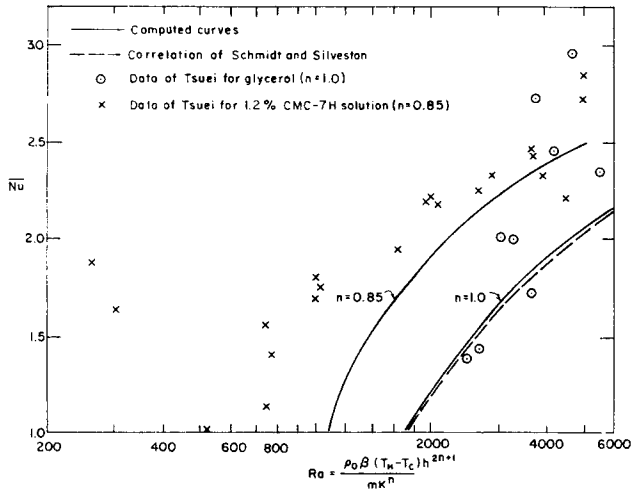

Fig. 19. Comparison of computed $\overline{Nu}$ for dragless vertical boundaries with experimental values.

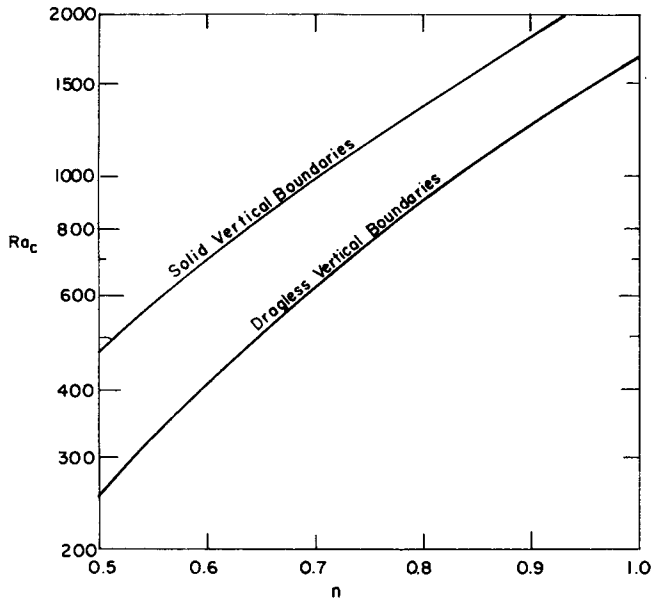

Fig. 20. Dependence of Ra_c on index of Ostwald-de Waele fluids for both solid and dragless vertical boundaries, $Pr > 1$

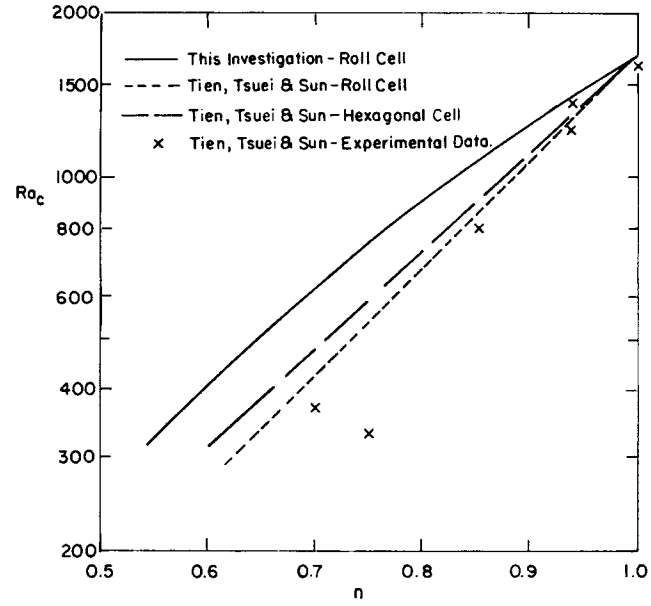

Fig. 21. Comparison of computed and experimental dependence of Ra_c on index of Ostwald-de Waele model for dragless vertical boundaries.

DISCUSSION

The computational procedures described herein can be used to calculate natural convection and hydrodynamic stability for a fluid heated below. Boundary conditions representing roll-cells with either solid or dragless vertical boundaries can be used. Test calculations were limited to the Ostwald-de Waele and Ellis models, but other models for pseudoplastic fluids can be used with only minor modification in the computer program. The computations become lengthy for the small grid-sizes required for convergence. Calculation of Nu at different levels as proposed by deVahl Davis does not obviate this difficulty. However, the results for relatively large grid-sizes can be extrapolated to zero grid-size with empirical correlations of the type presented herein. The program computes the transient as well as the steady behavior. The program is valid for all Pr but converges most rapidly for Pr near unity. The program was not tested for values of the Ostwald-de Waele index n less than 0.5, but would probably converge.

The correlation for the effect of grid size is based on only a few values for Newtonian fluids and Ostwald-de Waele fluids with $n = 0.5$. Its use appears to be confirmed for Newtonian fluids and dragless vertical boundaries by the improvement demonstrated between Figures 6 and 17. Its generality for solid vertical walls and for fluids with n other than 0.5 and 1.0 is unconfirmed because of the lack of reliable experimental data.

The computed values, extrapolated to zero grid-size, agree well with the experimental results for Newtonian fluids. The values computed for the Ostwald-de Waele model do not confirm the approximate solution of Tien, Tsuei, and Sun. Their experimental data are too scattered to evaluate the relative validity of these two predictions. Values computed for the Ellis model agree reasonably with the results for the equivalent Ostwald-de Waele model. Hysteresis was not observed in any of the calculations.

Retrospection on the results of this investigation with the help of excellent reviews suggests the following future work to refine and extend the results and to clarify aspects not yet resolved. A further experimental investigation of the effect of the width-to-height ratio on the critical Rayleigh number and on the Nusselt number for higher Rayleigh numbers appears desirable and indeed is currently in progress. It is hoped that heat leakage can be reduced and hence the accuracy of the heat transfer measurements improved by the use of guard cells rather than insulation in the continuing experimental work. In our future work as well as that of others, more precise and accurate experimental measurements are needed rather than just more data to test the predictions critically. It appears desirable to investigate experimentally and theoretically the effect of elasticity on the process in order to determine the limits of applicability of the results in that sense herein. It is also planned to investigate the use of several alternative finite-difference schemes which have recently been proposed in the hope of reducing the required computer time and hence making feasible extensive calculations with a smaller grid-size.

ACKNOWLEDGMENT

The authors acknowledge with thanks the very constructive criticisms provided by the reviewers. They deserve significant credit for improvement of the manuscript.

NOTATION

g = acceleration due to gravity, m/s^2
h = height of cell, m
H = $\eta K^{1-n}/mh^{2-2n}$ = dimensionless effective viscosity
k = thermal conductivity, W/m·°K
K = thermal diffusivity, m^2/s
l = width of cell, m
m = coefficient in Ostwald-de Waele model [Equation (5)], Ns^n/m^2
n = index in Ostwald-de Waele model [Equation (5)], dimensionless
$Nu(Y)$ = $q\ h/k(T_H - T_C)$ = Nusselt number computed at elevation Y
$\overline{Nu}(Y) = \frac{1}{l}\int_0^l Nu(Y)\,dx$ = average $Nu(Y)$ across cell
p = pressure, N/m^2
p' = $p - p_0 - g\rho_0\left(y - \frac{l}{2}\right)$ = dynamic pressure, N/m^2
P' = $p'h^{2n}/mK^n$ = dimensionless dynamic pressure
q = heat flux density in y-direction, J/s·m^2
Ra = $\rho_0 g\beta(T_H - T_C)h^{2n+1}/mK^n$ = Rayleigh number
Ra_c = critical value of Ra for transition between conductive and convective states
t = time, s
T = temperature, °K
T_C = temperature on upper surface ($y = 0$), °K
T_H = temperature on lower surface ($y = h$), °K
T_0 = $(T_H + T_C)/2$, °K
u = velocity component in x-direction, m/s
U = uh/K = dimensionless velocity component in x-direction
v = velocity component in y-direction, m/s
V = vh/K = dimensionless velocity component in y-direction
x = distance from left side of cell, m
X = x/h = dimensionless distance from left side of cell
y = distance from top of cell, m/s
Y = y/h = dimensionless distance from top of cell

Greek Letters

α = index in Ellis model [Equation (25)], dimensionless
β = volumetric coefficient of expansion with temperature, 1/°K
ζ = dimensionless vorticity [See Equation (21)]
η = effective viscosity, N·s/m^2
θ = $(T - T_0)/(T_H - T_C)$ = dimensionless temperature
μ = Newtonian viscosity, N·s/m^2
ρ = density, kg/m^3
σ = shear rate, N/m^2
τ = $t\ K/h^2$ = dimensionless time
τ^* = fictitious, dimensionless time used to solve Equation (21)
ϕ_0 = coefficient in Ellis model [Equation (25)], m^2/N·s
ϕ_1 = coefficient in Ellis model [Equation (25)], m$^{2\alpha}$/N$^\alpha$·s
Φ_0 = $\phi_0 mh^{2-2n}/K^{1-n}$ = coefficient in dimensionless form of Ellis model [Equation (26)]
Φ_1 = $\phi_1\ m^\alpha(h^2/K)^{1-n\alpha}$ = coefficient in dimensionless form of Ellis model [Equation (26)]
Ψ = dimensionless stream-function [See Equations (19) and (20)]

Subscripts

0 = at reference state ($T = T_0, p = p_0$)
X, Y, indicates partial differentiation

LITERATURE CITED

Aziz, K., and J. D. Hellums, "Numerical Solution of the Three Dimensional Equations of Motion for Laminar Natural Convection," *Phys. Fluids.*, **10**, 314 (1967).

Bird, R. B., W. E. Stewart and E. N. Lightfoot, *Transport Phenomena*, Wiley, New York (1960).

Brian, P. L. T., "A Finite-Difference Method of High-Order Accuracy for the Solution of Three-Dimensional Transient Heat Conduction Problems," *AIChE J.*, **7**, 367 (1961).

Chorin, A. J., "Numerical Study of Thermal Convection in a Fluid Layer Heated from Below," A.E.C. Research Develop. Report, NYO-1480-61, New York Univ. (1966).

Churchill, S. W. "The Prediction of Natural Convection," in. *Proc. of the Third Intern. Heat Transfer Conf.*, Vol. 6, p. 15, Am. Inst. Chem. Engrs., New York (1966).

deVahl Davis, G., private communication (1970).

Hellums, J. D., and S. W. Churchill, "Computation of Natural Convection by Finite Difference Methods," in *Intern. Developments in Heat Transfer*, Part V., p. 984, Am. Soc. Mech. Engrs., New York (1961).

———., "Transient and Steady State, Free and Natural Convection, Numerical Solutions: Part I. The Isothermal, Vertical Plate, Part 2. The region Inside a Horizontal Cylinder," *AIChE J.*, **8**, 690 (1962).

———., "Simplification of the Mathematical Description of Boundary and Initial Value Problems," *AIChE J.*, **10**, 110 (1964).

Kurzweg, U., "Convective Instability of a Hydromagnetic Fluid within a Rectangular Cavity," *Intern. J. Heat Mass Transfer*, **8**, 35 (1965).

Ozoe, H. "Hydrodynamic Stability of Non-Newtonian Fluids Heated from Below," Ph.D. thesis, Univ. Pennsylvania, Philadelphia (1971).

———., and S. W. Churchill, "Hydrodynamic Stability and Natural Convection in Newtonian and non-Newtonian Fluids Heated from Below," paper presented at 13th National Heat Transfer Conf., Denver, Colorado (1972).

———., "Natural Convection in non-Newtonian Fluids Heated from Below," paper presented at First Pacific Chem. Eng. Congr. (1972).
Samuels, M. R., "Stability of a Fluid in a Long Horizontal, Rectangular Cylinder Heated from Below," Ph.D. thesis, Univ. Michigan, Ann Arbor (1966).
———., and S. W. Churchill, "Stability of a Fluid in a Rectangular Region Heated from Below," *AIChE J.*, **13**, 77 (1967).
Schmidt, E., and P. L. Silveston, "Natural Convection in Horizontal Liquid Layers," *Chem. Eng. Progr. Symp. Ser. No. 29*, **55**, 163 (1959).
Thomas, R. W., "Finite Difference Computation of Heat Transfer by Natural Convection," Ph.D. thesis, Univ. New South Wales, Australia (1970).
Tien, C., H. S. Tsuei, and Z. S. Sun, "Thermal Instability of a Horizontal Layer of non-Newtonian Fluid Heated from Below," *Intern. J. Heat Mass Transfer*, **12**, 1173 (1969).
Tsuei, H. S., "Thermal Instability and Heat Transport of a Layer of non-Newtonian Fluid," Ph.D. thesis, Syracuse Univ. New York (1970).
Wikes, J. O., and S. W. Churchill, "The Finite-Difference Computation of Natural Convection in a Rectangular Enclosure," *AIChE J.*, **12**, 161 (1966).

Manuscript received November 11, 1971; revision received June 21, 1972; paper accepted July 10, 1972.

The Optimal Control of a Periodic Adsorber:

DANIEL E. KOWLER and ROBERT H. KADLEC

Department of Chemical Engineering
The University of Michigan, Ann Arbor, Michigan 48104

Part I. Experiment

Cyclic pressure variations in a fixed bed adsorber can cause significant separation of gaseous mixtures. Feed pressure changes are the driving force in this parametric pumping process. The optimal feed sequence is maximum (maximum flow in) pressure, zero flow (variable pressure), maximum flow out (minimum pressure). For the nitrogen-methane feed gas at 168 k N/m^2 and a 1.22 m bed of adsorbent, the optimal cycle time is 3 seconds, and feed is sustained 50% of the time. The zero flow mode is unnecessary if product purity is the sole objective.

SCOPE

The components of a binary gas mixture exhibit different adsorption characteristics on a solid adsorbent such as a molecular sieve, the difference usually being expressed as a relative volatility. If such a mixture is steadily passed through a fixed bed of adsorbent particles, the adsorbed phase will adjust to a composition which is consistent with the equilibrium adsorption isotherms for the system for the given feed composition and the bed temperature. Under such a steady flow condition, no separation of the mixture occurs after the adsorbent is loaded.

If the feed pressure is alternated between values higher and lower than the bed entrance pressure, a feed flow will alternate with feed-end exhausting of the bed. This can be done while continuously withdrawing gas at the product end of the bed. If such cycling is continued until each cycle is like the previous, the product gas is enriched in the least strongly adsorbed component.

The system will not separate if run exclusively at the maximum feed rate or at the minimum (negative) feed rate, thus an optimum feed-exhaust policy must exist. Furthermore, if the cycle time is too short, the bed sees a mean inlet feed pressure, and no separation occurs. Likewise, an infinitely slow cycle time means steady operation, and again, no separation. Thus an optimum cycle time exists. The objectives of the optimization can be either product purity or capacity, or a combination of both.

The scope of Part I of this paper is the determination of the experimental optimum pressure wave form and cycle time for the methane-nitrogen-molecular sieve system. The theory of Part II indicates that the family of square waves encompasses the optima for a system in dynamic equilibrium. Therefore, the variables of cycle time, % of time at maximum feed pressure, no feed flow, and minimum (exhaust) feed pressure were experimentally explored. Other quantities, such as bed length and diameter, feed composition, temperature and molecular sieve parameters, were not varied.

The model of this system was previously developed for the instantaneous equilibrium assumption and is employed here. The theoretical optimization procedures were both an analysis of the model partial differential equations and an extension of the procedure of Horn and Lin, based on the Pontryagin Maximum Principle.

Hence, the scope of this work includes the experimental

Correspondence concerning this paper should be addressed to R. H. Kadlec.